# PAPER

Check for updates

# Bioactive polyphenols from *Isodon serra* with antioxidant and hepatoprotective activities *in vitro* and *in vivo*

Siqin Li,†[ab] Ziying Huang,†[a] Lin Lv,[a] Shixiong Wang,[a] Guang Yang,[c] Linjie Zhang,[c] Mengyao Du,[d] Yi Zhang,[a] Jiang Ma,[a] Min Hong,[e] Xin He [ID] *[a] and Ji Yang [ID] *[a]

*Isodon serra* is a medicinal plant with notable antioxidant potential underlying its hepatoprotective properties, suggesting the presence of highly active antioxidant constituents. To identify these bioactive components, the target compounds were isolated and structurally elucidated using chromatographic and spectroscopic techniques. Antioxidant activities were evaluated using DPPH radical scavenging and ferric reducing antioxidant power (FRAP) assays, together with *tert*-butyl hydroperoxide (*t*-BHP)-induced oxidative stress models *in vitro* and *in vivo*. As a result, ten monomeric compounds were isolated from *I. serra*, including two new compounds, labiserins A (**1**) and B (**2**), which were identified as a carboxylated α-pyrone derivative and a dihydrobenzofuran neolignan, respectively. Compound **7** showed the highest potency ($EC_{50} = 10.9 \pm 0.4$ μM), which was nearly tenfold lower than that of vitamin C ($EC_{50} = 101.1 \pm 3.1$ μM). In HepG2 cells, **7** dose-dependently attenuated *t*-BHP-induced cell death, while significantly reducing intracellular reactive oxygen species (ROS) and malondialdehyde (MDA) levels and enhancing superoxide dismutase (SOD) activity. qRT-PCR analysis indicated that its hepatoprotective effect is associated with transcriptional modulation of Keap1 and suppression of NF-κB-mediated inflammatory responses. In mice, **7** significantly reduced serum alanine aminotransferase (ALT) and aspartate aminotransferase (AST) levels, diminished hepatic MDA accumulation, and ameliorated *t*-BHP-induced histopathological liver damage. Collectively, these findings reveal new antioxidant polyphenols from *I. serra* and identify **7** as a potent hepatoprotective constituent *in vitro* and *in vivo*.

## Introduction

Due to its central role in metabolism, the liver is particularly vulnerable to oxidative stress, a major driver of the onset and progression of liver diseases.[1] Excessive reactive oxygen species (ROS) not only damage cellular macromolecules but also disrupt redox homeostasis through Nrf2/Keap1 imbalance, thereby activating pro-inflammatory pathways (*e.g.*, NF-κB, TNF-α, IL-6) and Kupffer cells.[2] The resulting persistent inflammation stimulates hepatic stellate cells *via* profibrogenic mediators such as TGF-β and PDGF, leading to extracellular matrix accumulation, fibrosis, and ultimately cirrhosis and hepatocellular carcinoma.[3] Given that oxidative stress acts as the initiating

switch of liver pathogenesis, targeting it has become a critical strategy for prevention and therapy.[4]

Natural polyphenols are a diverse group of plant secondary metabolites characterized by multiple phenolic hydroxyl groups, which confer strong antioxidant capacity through free radical scavenging and metal ion chelation.[5] More importantly, they mitigate oxidative stress by enhancing endogenous antioxidant defenses and modulating redox-sensitive signaling pathways such as Nrf2/Keap1 and NF-κB, thereby exerting hepatoprotective effects.[6] Silibinin, a flavonolignan isolated from the seeds of *Silybum marianum*, has been applied as a hepatoprotective agent, exerting its effects by lowering intracellular ROS levels, reducing MDA accumulation, and enhancing glutathione peroxidase (GSH-Px) activity.[7] Hydroxytyrosol, a major olive polyphenol, has been reported to significantly reduce serum ALT and AST levels, suppress inflammation, and attenuate oxidative stress in a mouse model of acute liver injury.[8] The significant bioactivities of natural polyphenols have stimulated increasing efforts to discover novel hepatoprotective agents from medicinal plants.

*Isodon serra* (Maxim.) Hara, belonging to the family Lamiaceae, is mainly distributed in tropical and subtropical Asia. In southern China, the aerial parts of *I. serra* have been traditionally used as a folk medicine for the treatment of acute jaundice, hepatitis, and

*[a] School of Traditional Chinese Materia Medica, Guangdong Pharmaceutical University, Guangzhou 510006, China. E-mail: hexintn@163.com; yangji@gdpu.edu.cn*

*[b] Department of Pharmacy, Shaoguan First People's Hospital, Affiliated Hospital of Shaoguan University, Shaoguan 512000, China*

*[c] China Academy of Chinese Medical Sciences, Beijing 100700, China*

*[d] Hebei University of Traditional Chinese Medicine, Shijiazhuang 050200, China*

*[e] The First Affiliated Hospital of Guangdong Pharmaceutical University, Guang Dong 510080, China*

† These authors have contributed equally to this work.

acute cholecystitis.[9] Previous phytochemical investigations were primarily centered on *ent*-kaurane diterpenoids in low-polarity fractions due to their structural variability and potent anticancer bioactivities.[10,11] By contrast, although the high-polarity aqueous extract of *I. serra* is clinically used for hepatoprotection, its chemical profile and pharmacological relevance have yet to be clearly elucidated.[12] Although some phenolic compounds have been identified in the aqueous extract, the hepatoprotective effects of the aqueous extract and active constituents remain insufficiently characterized. Therefore, it is of significant importance to elucidate the material basis of its hepatoprotective activity and identify potential active compounds responsible for this effect.

To elucidate the material basis of its hepatoprotective activity and to identify antioxidant lead compounds, this study isolated and characterized the polyphenolic fraction of *I. serra* and evaluated its hepatoprotective effects *in vitro* and *in vivo*.

# Results and discussion

### Antioxidant assays of different parts of *I. serra*

Phenolic compounds may directly contribute to antioxidant action because of their redox properties. These compounds can act on the antioxidant defense system and alleviate oxidative stress.[13] The higher the phenolic and flavonoid contents, the stronger the antioxidant activity. As shown in Fig. 1a, it could be noted that the TP fraction exhibited the highest TPC with a value of $291.9 \pm 6.5$ mg GAE per g. In contrast, the PE fraction showed the lowest TPC with a value of $57.2 \pm 3.7$ mg GAE per g. The remaining fractions followed in the order of EE, EA, and AS fractions with closely comparable values of $112.7 \pm 0.2$, $105.6 \pm 0.2$, and $93.0 \pm 0.6$ mg GAE per g, respectively. These values indicated that the TP fraction possessed strong antioxidant activity owing to high contents of phenolic compounds.

DPPH is widely used as a standard method for evaluating the free radical scavenging capacity of antioxidants.[14] The FRAP assay quantifies the antioxidative capacity of any substance in the reaction medium as a reducing ability. The obtained fractions (EE, PE, EA, AS, and TP) were evaluated for their antioxidant activities by DPPH and FRAP assays. As illustrated in Fig. 1b and c, the TP fraction exhibited significantly stronger antioxidant activity compared to the other fractions. In the DPPH assay, the TP fraction expressed the highest inhibition

percentage with values of $28.74 \pm 0.76\%$, followed by EA, AS, EE, and PE with values of $17.91 \pm 1.15\%$, $14.25 \pm 2.47\%$, $11.03 \pm 1.82\%$, and $7.18\% \pm 2.09\%$, respectively. Similarly, in the FRAP assay, the TP fraction demonstrated the best total antioxidant capacity with $3.4 \pm 0.2$ mmol $Fe^{2+}$/mg, followed by EA, EE, AS, and PE with values of $1.73 \pm 0.16$, $1.39 \pm 0.09$, $1.42 \pm 0.03$, and $0.49 \pm 0.04$ mmol $Fe^{2+}$/mg, respectively. This biological activity is consistent with the TPC content, and the TP fraction of *I. serra* 's antioxidant activity has been attributed to its phenolic compounds, which are more abundant in the TP fraction.

### Cytotoxicity and cytoprotective effects of different parts of *I. serra*

To ensure that the different parts of *I. serra* used in subsequent experiments were not toxic to cells, it was necessary to determine cytotoxicity. As shown in Fig. 2a, the EE and EA parts exhibited significant inhibitory effects against HepG2 cells ($p < 0.01$), while the EE, AS, and TP parts treated groups exhibited no toxicity. Thus, the EE, AS, and TP parts were selected for further experiments. Cells were cultured with *t*-BHP (0–500 μM) for 2 h to clarify the cytotoxicity of *t*-BHP. After treatment, the viability of HepG2 cells reduced significantly in a concentration-dependent manner, indicating that the *t*-BHP-induced HepG2 cells oxidative damage model was successfully constructed.[15,16] At 300 μM *t*-BHP, cell viability decreased to 50% (Fig. 2b). Subsequently, 300 μM *t*-BHP was selected as the concentration for further oxidative damage experiments. The cytoprotective effect of EE, AS, and TP parts against *t*-BHP (300 μM, 2 h) induced cytotoxicity was shown in Fig. 2c. Results indicated that the TP parts showed a significant protective effect against hepatotoxicity induced by *t*-BHP ($p < 0.01$), and the effect was better than EE and AS fractions, confirming that phenolic compounds underpin the hepatoprotective activity *via* antioxidant action of the *I. serra* aqueous extract.

### Isolation, identification, and characterization of the TP fraction from *I. serra*

Phytochemical investigation of the active fraction (TP) from *I. serra* led to the isolation of two new polyphenols (**1** and **2**), together with eight known compounds (**3–10**) (Fig. 3).
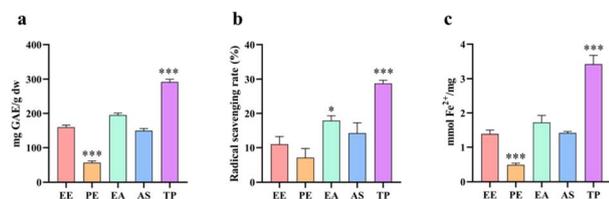


Fig. 1 The activity of five fractions of *I. serra* was evaluated. (a) The total phenols content (TPC) is expressed as gallic acid equivalents (GAE) of the dry weight sample. (b) DPPH free radical scavenging activity. (c) Ferric reducing antioxidant power (FRAP). EE, ethanol extract; PE, petroleum ether; EA, ethyl acetate; AS, aqueous solution; TP, total polyphenols. The data were expressed as means $\pm$ SD ($n = 3$). *$p < 0.05$, **$p < 0.01$, and ***$p < 0.001$ *versus* the EE group.
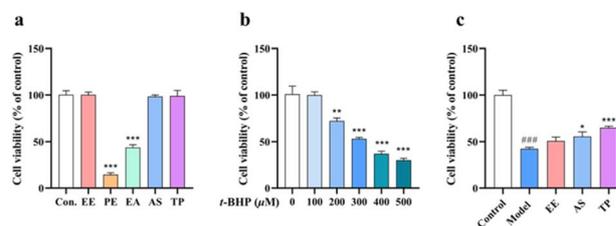


Fig. 2 Cytotoxicity and the cytoprotective effects of different parts of *I. serra*. (a) Cell viability of HepG2 cells treated with 50 μg mL$^{-1}$ different parts of *I. serra* for 24 h. (b) Cell viability following treatment with *t*-BHP (0–500 μM) for 2 h. (c) Cell viability of HepG2 cells was pretreated with or without 50 μg mL$^{-1}$ EE, AS, and TP parts for 24 h, and then incubated with or without *t*-BHP (300 μM) for 2 h. The data were expressed as means $\pm$ SD ($n = 3$). #$p < 0.05$, ##$p < 0.01$, and ###$p < 0.001$ *versus* the control group. *$p < 0.05$, **$p < 0.01$, and ***$p < 0.001$ *versus* the model group.
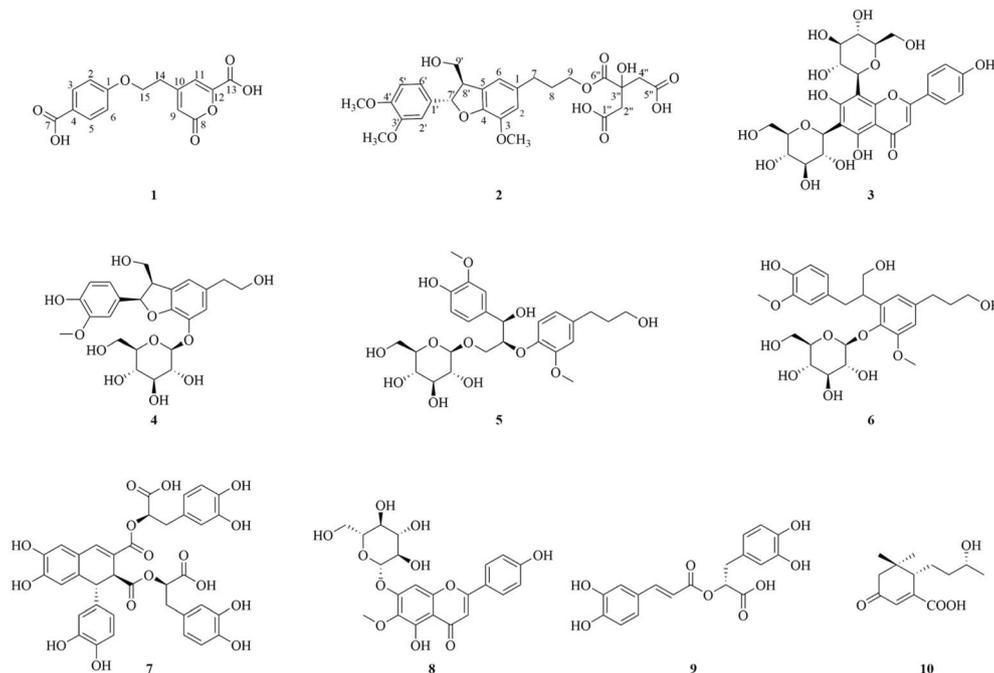
**Fig. 3** Chemical structures of **1–10**.

Compound **1** was obtained as a white amorphous powder. The IR spectrum showed a broad absorption peak at 3400 cm$^{-1}$ for hydroxy, an intense band at 1720 cm$^{-1}$ for carbonyl functional groups, and 1608 cm$^{-1}$ for double bonds. The $^1$H NMR spectrum (Table 1) exhibited one olefinic proton at $\delta_H$ 6.34 (1H, s) and a group of AB coupling aromatic protons at $\delta_H$ 7.81 (1H, d, $J$ = 8.6 Hz) and 6.81 (1H, d, $J$ = 8.6 Hz). Analyses of $^{13}$C, DEPT, and HSQC experiments revealed the existence of 15 carbons, including seven quaternary carbons, six methines, and two methylene groups. The above data of **1** (Table 1) closely resembled those of dumortins B,[17] except that a phenolic *ortho*-dihydroxy group ($\delta_C$ 143.4 and 144.9) in dumortins B was replaced by a carboxylic acid ($\delta_C$ 162.3) in **1**, and a methylene ($\delta_C$ 35.9) in dumortins B was substituted by an oxygenated methylene ($\delta_C$ 62.0). This hypothesis was confirmed by the HMBC correlations of H-3/H-5 with C-7, H-2/H-4 with C-6, and H-15/H-12 with C-1(Fig. 4a). Its molecular formula was assigned to be C$_{15}$H$_{12}$O$_7$ with ten degrees of unsaturation by the HR-ESI-MS ion at $m/z$ 305.0657 [M + H]$^+$ (Calculated for C$_{15}$H$_{13}$O$_7$, 305.0656). Thus, the structure of **1** was identified and named as labiserin A.

Compound **2** was obtained as a pale yellowish amorphous powder with the molecular formula of C$_{27}$H$_{32}$O$_{12}$ according to the HR-ESI-MS spectrum at $m/z$ 571.1783 [M + Na]$^+$ (Calculated for C$_{27}$H$_{32}$O$_{12}$Na, 571.1785), corresponding to 12 degrees of unsaturation. The $^1$H NMR spectrum (Table 1) indicated the existence of three methyls at $\delta_H$ 3.86 (3H, s), 3.81 (3H, s), and 3.79 (3H, s), as well as five aromatic protons at $\delta_H$ 6.93 (1H, dd, $J$ = 1.7, 1.8 Hz), 6.92 (1H, s), 6.73 (1H, s), 6.74 (1H, s), and 6.97 (1H, d, $J$ = 1.7 Hz). The $^{13}$C, DEPT, and HSQC NMR spectra of **2** revealed 27 carbons, including three methyls, seven methines, six methylenes, and eleven quaternary carbons (Table 1). A careful analysis of the 1D NMR data of **2** revealed it is very

similar to 3′,4-O-dimethylcedrusin,[18] except for an additional moiety attached at C-9 ($\delta_C$ 65.1). This additional moiety was superimposable on those of 2-Hydroxy-4-oxo-2-(2-oxopropyl) pentanoic acid, and the major difference was that the two methyl groups were replaced by two hydroxy groups. This hypothesis was confirmed by key HMBC correlations of H-2″ ($\delta_H$ 2.80) to C-1as well as H-4″ ($\delta_H$ 2.93) to C-5″. The HMBC cross-peak from H-9 to C-6″ indicated that the additional moiety was located at the C-9 position (Fig. 4a). The correlation of H-7′ and H-9′ determined that H-7 was in the $\alpha$-orientation and H-8 was in the $\beta$-orientation (Fig. 4b). The absolute configuration of (7′S, 8′R)-**2** was determined by comparing its experimentally obtained ECD spectrum with the theoretically calculated ECD spectra, as illustrated in Fig. 4c. Hence, the structure of **2** was identified and named as labiserin B.

The known compounds were identified by comparing their spectroscopic data with those reported in the literature as vicenin II (**3**),[19] umbroside (**4**),[20] camellignanoside A (**5**),[21] icariside E3 (**6**),[22] rabdosiin (**7**),[23] homoplantaginin (**8**),[24] rosmarinic acid (**9**),[25] and 1,3-carboxyblumenol C (**10**).[26]

To investigate the chemical characteristics of the most bioactive fraction used in the present study, HPLC analysis of the TP fraction was carried on, and all isolated compounds were identified based on the chromatographic analysis (Fig. 5). The findings revealed that the principal chromatographic peak was assigned as **7** with 17.3% constitution in the TP fraction.

## Antioxidant activities of isolated compounds from the TP fraction of *I. serra*

The isolated compounds (**1–10**) from the TP of *I. serra* were evaluated for their antioxidant activities using DPPH radical scavenging and FRAP assays (Fig. 6a and b). In the DPPH assay,

**Table 1** $^1$H NMR (600 MHz) and $^{13}$C NMR (150 MHz) spectroscopic data of **1** and **2** ($\delta$ in ppm, $J$ in Hz)

| Position | 1 (in MeOD) | | Position | 2 (in MeOD) | |
|---|---|---|---|---|---|
| | $\delta_C$ (type) | $\delta_H$ (mult., $J$ in Hz) | | $\delta_C$ (type) | $\delta_H$ (mult., $J$ in Hz) |
| 1 | 166.5 (C) | | 1 | 136.3 (C) | |
| 2 | 114.9 (CH) | 6.81 (d, 8.6) | 2 | 118.1 (CH) | 6.73 (s) |
| 3 | 131.4 (CH) | 7.84 (d, 8.6) | 3 | 145.6 (C) | |
| 4 | 120.4 (C) | | 4 | 147.7 (C) | |
| 5 | 131.4 (CH) | 7.84 (d, 8.6) | 5 | 129.8 (C) | |
| 6 | 114.9 (CH) | 6.81 (d, 8.6) | 6 | 114.2 (CH) | 6.74 (s) |
| 7 | 162.3 (C) | | 7 | 32.8 (CH$_2$) | 2.65 (t, 7.5) |
| 8 | 163.2 (C) | | 8 | 31.7 (CH$_2$) | 1.92 (m) |
| 9 | 114.7 (CH) | 6.34 (s) | 9 | 65.1(CH$_2$) | 4.07 (t, 6.3) |
| 10 | 157.5 (C) | | 1′ | 136.3(C) | |
| 11 | 109.1 (CH) | 7.08 (s) | 2′ | 110.7 (CH) | 6.97 (d, 1.7) |
| 12 | 155.1 (C) | | 3′ | 150.6 (C) | |
| 13 | 164.0 (C) | | 4′ | 150.2 (C) | |
| 14 | 34.0 (CH$_2$) | 2.98 (t, 6.1) | 5′ | 112.9 (CH) | 6.92 (s) |
| 15 | 62.0 (CH$_2$) | 4.53 (m) | 6′ | 119.4 (CH) | 6.93 (dd, 1.7, 1.8) |
| | | | 7′ | 88.7 (CH) | 5.53 (d, 6.1) |
| | | | 8′ | 55.4 (CH) | 3.46 (m) |
| | | | 9′a | 65.1 (CH$_2$) | 3.84 (overlap) |
| | | | 9′b | | 3.75 (dd, 7.4, 11.1) |
| | | | 1″ | 177.1 (C) | |
| | | | 2″ | 44.4 (CH$_2$) | 2.93 (m) |
| | | | 3″ | 74.3 (C) | |
| | | | 4″ | 44.4 (CH$_2$) | 2.80 (m) |
| | | | 5″ | 173.8 (C) | |
| | | | 6″ | 171.7 (C) | |
| | | | 4′-OCH$_3$ | 56.5 (CH$_3$) | 3.81 (s) |
| | | | 3′-OCH$_3$ | 56.5 (CH$_3$) | 3.79 (s) |
| | | | 3-OCH$_3$ | 56.9 (CH$_3$) | 3.86 (s) |

7 showed the best radical scavenging activity with an EC$_{50}$ value of 10.9 ± 0.4 μM, which was nearly tenfold higher than that of vitamin C (EC$_{50}$ = 101.1 ± 3.1 μM). Compound **9** also demonstrated stronger scavenging activity than vitamin C with EC$_{50}$ values of 66.1 ± 2.7 μM. The remaining compounds all demonstrated similar and limited scavenging activity, even at 200 μM. In the FRAP assay, **7** and **9** exhibited strong ferric-reducing abilities, with values of 11.78 ± 1.3 and 11.05 ±
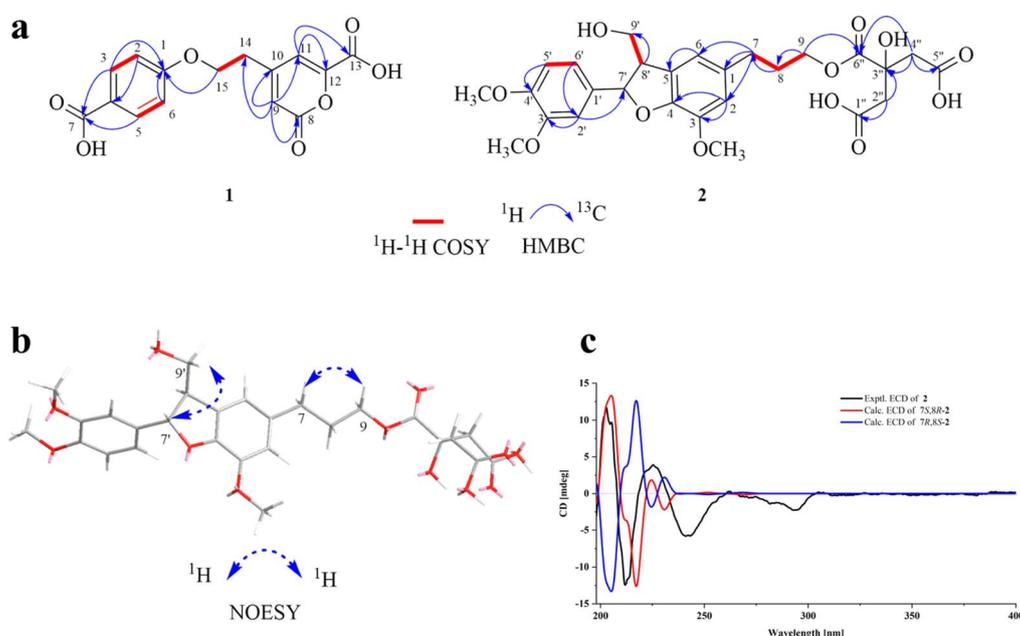


**Fig. 4** (a) $^1$H–$^1$H COSY and key HMBC correlations of **1** and **2**. (b) Key NOESY correlations of **2**. (c) Experimental and calculated ECD spectra of **2**.
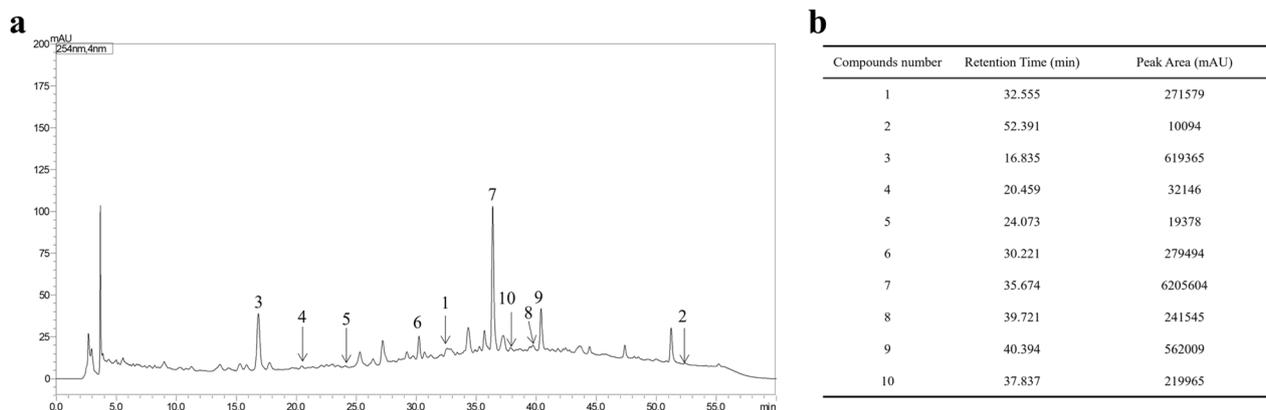
**Fig. 5** Characterization of the TP fraction of *l. serra*. (a) HPLC-UV chromatograms and identification of chromatographic peaks. (b) Details regarding the retention time and peak area for each component corresponding to the chromatographic peaks.
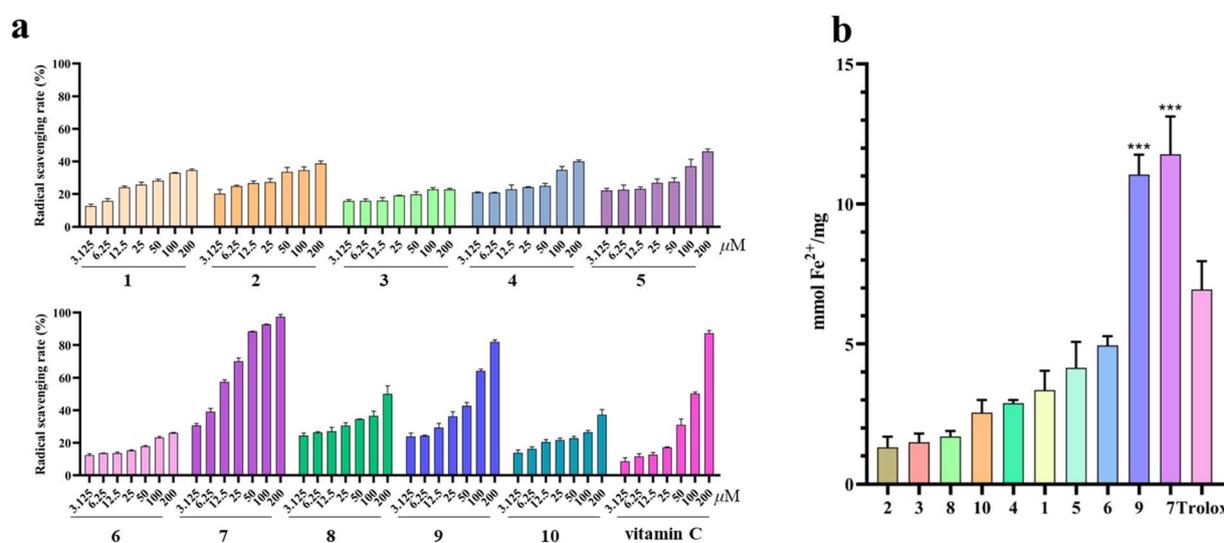


**Fig. 6** Antioxidant activities of isolated compounds from the TP fraction of *l. serra*. (a) The DPPH radical scavenging assay. (b) The ferric-reducing antioxidant power assay. The data were expressed as means $\pm$ SD ($n = 3$). *$p < 0.05$, **$p < 0.01$, and ***$p < 0.001$ *versus* the positive group.

0.71, both of which were higher than that of the positive control Trolox ($6.94 \pm 0.83$).

Antioxidant capacity is often considered an indicator of the bioactivity of medicinal plant constituents.[27] Previous studies have reported that caffeic acid derivatives possess strong antioxidant activities.[28] In our research, 7 and 9 stood out as the two most potent antioxidants among the isolated polyphenols.[29] Structurally, 9 was identified as rosmarinic acid. Essentially, it can be regarded as a dimeric derivative of caffeic acid composed of an ester linkage between caffeic acid and 3,4-dihydroxyphenyllactic acid, containing two catechol moieties capable of donating hydrogen atoms to neutralize free radicals.[30] 7, a dimeric analogue of 9 (rosmarinic acid), possesses a more complex polyphenolic scaffold with multiple caffeoyl moieties.[31] The significantly enhanced antioxidant potency of the dimeric 7, relative to the monomeric analogue 9, can be primarily attributed to the presence of two catechol moieties within its structure. Catechol groups are well recognized for

their radical-scavenging capability *via* hydrogen atom transfer and single-electron transfer mechanisms, and the incorporation of dual catechol units in 7 provides an inherent stoichiometric advantage, enabling a single molecule to neutralize a greater number of free radicals.[32] In addition to this quantitative effect, the intramolecular proximity of the two catechol groups may facilitate electronic interactions that stabilize the phenoxyl radical intermediate generated after the initial scavenging event.[33] Such stabilization could lower the energetic cost of radical quenching, thereby rendering 7 a more efficient antioxidant than 9, which contains only a single catechol unit.

## The protective effects of 7 against *t*-BHP-induced hepatotoxicity *in vitro*

The cytotoxicity of 7 against HepG2 cells was assessed *via* the MTT assay. Cells were treated with 7 at concentrations of 0–320 $\mu$M for 24 h, and its $IC_{50}$ value was greater than 320 $\mu$M (Fig. 7a). Within the concentration range of 0–80 $\mu$M, 7 did not exhibit
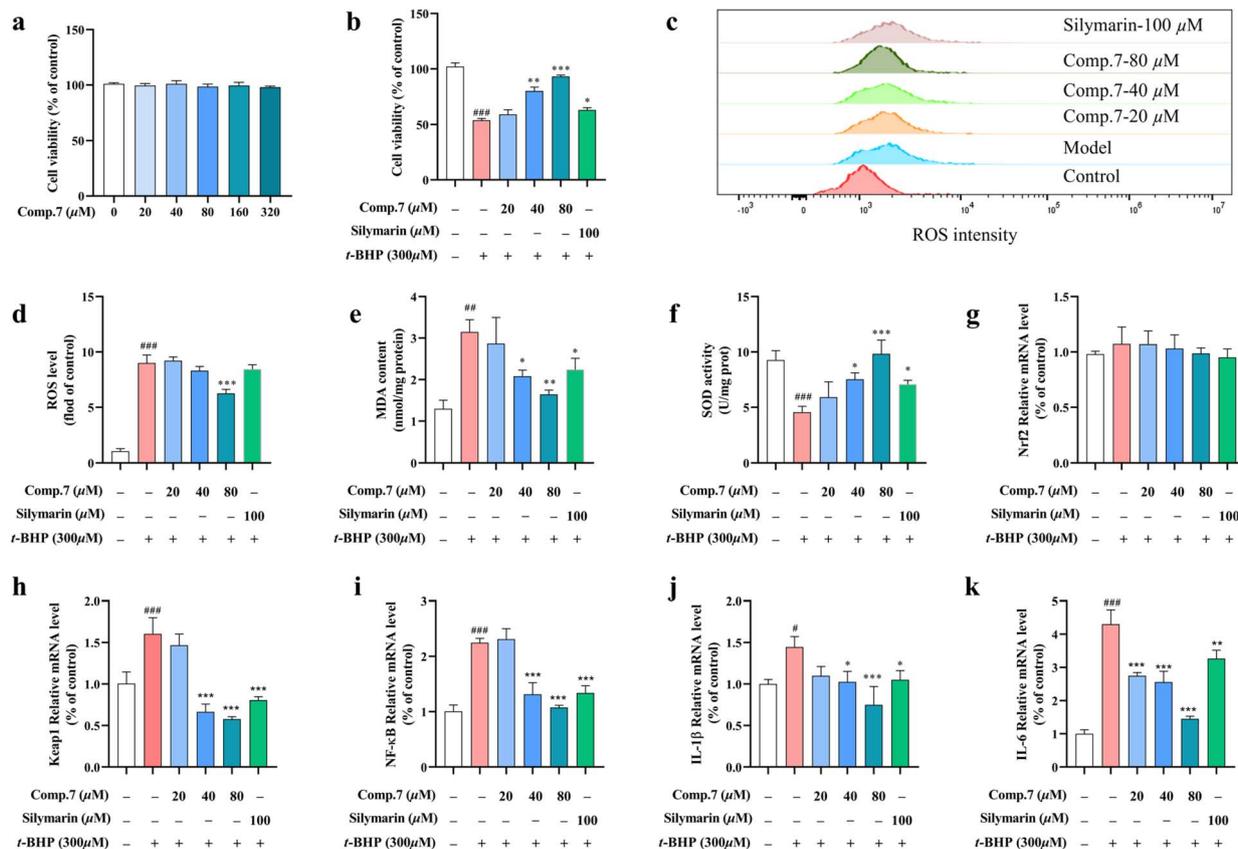
Fig. 7  Effects of 7 on *t*-BHP-induced oxidative stress *in vitro*. (a) Cell viability following treatment with 7 (0–320 μM) for 24 h. (b) Cell viability of HepG2 cells pretreated with 7 (0, 20, 40, and 80 μM) or silymarin (100 μM) for 24 h before exposure to *t*-BHP (300 μM) for 2 h. (c) Intracellular ROS levels were analyzed by flow cytometry. (d) Quantification analysis of ROS levels. (e and f) MDA levels and SOD activity of HepG2 cells exposed to 7 (0, 20,40, and 80 μM) for 24 h and then incubated with *t*-BHP (300 μM) for 2 h. (g–k) HepG2 cells were pre-incubated with 7 (0, 20, 40, and 80 μM) or silymarin (100 μM) for 24 h before exposure to *t*-BHP (300 μM) for 2 h. The mRNA levels of Nrf2, Keap1, NF-κB, IL-1β, and IL-6 were measured by qRT-PCR. The data shown represent the mean values of three experiments ± SD. #$p < 0.05$, ##$p < 0.01$, and ###$p < 0.001$ *versus* the control group. *$p < 0.05$, **$p < 0.01$, and ***$p < 0.001$ *versus* the model group.

cytotoxicity compared with the control group. Thus, different concentrations of 7 (20, 40, and 80 μM) were selected for further experiments. The cytoprotective effect of 7 against *t*-BHP-induced cytotoxicity was analyzed by determining cell viability. HepG2 cells were pretreated with 7 (0–80 μM) for 24 h and then exposed to *t*-BHP for another 2 h. Results (Fig. 7b) indicated a higher dose of 7 (80 μM) further reduced cell damage to values similar to those of control cells, indicating the potent protective activity of 7 against *t*-BHP-induced cytotoxicity in HepG2 cells. Notably, at concentrations of 40 and 80 μM, 7 exhibited hepatoprotective effects that were superior to those of the positive control silymarin tested at 100 μM.

The excessive production of reactive oxygen species (ROS) plays a pivotal role in the pathogenesis of cellular oxidative stress injury.[34] To verify that 7 attenuated *t*-BHP-induced oxidative stress in HepG2 cells, ROS levels were measured by a DCFH-DA probe. As can be seen from Fig. 7c and d, a dramatic increase in the ROS content was noted in HepG2 cells after treatment with *t*-BHP for 2 h ($p < 0.01$). However, 7 pretreatments decreased the ROS content in a dose-dependent manner. The measurement of MDA, as a biomarker for lipid peroxidation, can indirectly reflect the extent of cellular damage.[35]

The effects of 7 on *t*-BHP-induced MDA generation are shown in Fig. 7e. In this study, *t*-BHP significantly increased the MDA level in HepG2 compared to the control group ($p < 0.01$). However, pretreatment of HepG2 cells with 7 remarkably decreased the intracellular MDA level at 40 and 80 μM ($p < 0.05$ and 0.01, respectively). The above results indicate that 7 possesses the ability to inhibit the elevation of MDA level and ameliorate HepG2 cell damage, thereby exhibiting an anti-oxidative effect.

The SOD activity was assessed as an indicator of the enzymatic antioxidant defense system in HepG2 cells under conditions of oxidative stress.[36] The effects of 7 on *t*-BHP-induced SOD depletion are shown in Fig. 7f. SOD activity was notably lower by 50.8% in HepG2 cells treated with 300 μM *t*-BHP alone (model group) compared to the control group ($p < 0.01$). On the contrary, pretreatment with different concentrations of 7 significantly reversed the phenomenon ($p < 0.01$). The data indicate that 7 exerts its protective effects by enhancing the cellular antioxidant capacity.

To explore the potential mechanism underlying the hepatoprotective effects of 7, qRT-PCR analysis was performed to assess the transcriptional expression of multiple oxidative

stress-and inflammation-related genes, including Nrf2, Keap1, NF-κB, IL-6, and IL-1β. The results showed that the total mRNA expression level of Nrf2 in HepG2 cells exhibited no significant change following *t*-BHP treatment, and pretreatment with 7 or silymarin did not alter its transcriptional level. In parallel, Keap1 mRNA expression was markedly increased in response to *t*-BHP exposure, whereas pretreatment with 7 or silymarin reduced Keap1 expression in a dose-dependent manner (Fig. 7g and h). Notably, *t*-BHP exposure led to a pronounced upregulation of NF-κB as well as the pro-inflammatory cytokines IL-6 and IL-1β at the mRNA level, whereas pretreatment with 7 significantly attenuated these increases in a dose-dependent fashion, comparable to the effects observed with silymarin (Fig. 7i–k).

Previous studies have established that Keap1 is a key negative regulator of cellular antioxidant responses and has also been implicated in the modulation of inflammatory signaling.[37] In the present study, although the total mRNA expression level of Nrf2 remained unchanged, Keap1 transcription was significantly upregulated under *t*-BHP-induced oxidative stress and was effectively downregulated by pretreatment with 7.[38] Given the central role of Keap1 at the interface of redox homeostasis and inflammatory regulation, its transcriptional modulation may contribute to the coordinated attenuation of oxidative stress-associated inflammatory responses.[39] Consistent with this notion, 7 markedly inhibited NF-κB activation and reduced the expression of pro-inflammatory cytokines IL-6 and IL-1β, suggesting that the concurrent modulation of oxidative stress and inflammation *via* Keap1 represents an important component of its hepatoprotective mechanism. In a previous study, it was demonstrated that 7 is a potent scavenger of active oxygen species, such as superoxide anion radicals and hydroxyl radicals.[40] However, to the best of our knowledge, there are no studies available to date on the effects of 7 on *t*-BHP-induced oxidative stress in liver cells. Thus, the present study suggests that 7 protects cells from *t*-BHP-induced oxidative damage more

effectively than silymarin by inhibiting the production of ROS, reducing MDA levels, and enhancing SOD activity. Furthermore, these findings clarify that its hepatoprotective effect is associated with transcriptional modulation of Keap1 and the inhibition of the NF-κB inflammatory response. Additionally, it was also indicated that 7 is the bioactive compound responsible for the hepatoprotective properties of the TP fraction of *I. serra*.

## The protective effects of 7 against *t*-BHP-induced hepatotoxicity *in vivo*

The hepatoprotective effects of 7 were also investigated in *t*-BHP-induced liver injury mice. H&E staining revealed marked differences in histopathological liver injury among different groups of mice. As shown in Fig. 8a, normal mice that were not exposed to *t*-BHP exhibited a well-preserved cellular distribution with a clear distinction of cells. However, *t*-BHP injection caused ballooned hepatocytes, inflammatory cell infiltrations, and obscure cell boundaries. Pretreatment with 7 efficiently aggravated these features, and the high-dose group showed a similar tissue structure to that observed in the normal group. A significant reduction was observed in the histopathological score in the Comp.7 H group in comparison to that of the model group ($p < 0.01$) (Fig. 8b). As shown in Fig. 8c, in comparison with the control group, the model group gained a significant increase in liver index ($p < 0.01$). Interestingly, the pretreatment with a high dose of 7 significantly attenuated the *t*-BHP-induced elevation in the liver index ($p < 0.01$). These data indicated that 7 protected the liver from *t*-BHP-induced histopathology. The hepatic enzymes ALT and AST in serum were utilized as the biochemical markers for early acute hepatic damage. As depicted in Fig. 8d and e, the *t*-BHP-treated animals showed a noticeable increase in the activity of ALT and AST ($p < 0.01$), in comparison with the normal group. In contrast, pretreatment with 7 distinctly suppressed the increase of ALT and AST levels induced by *t*-BHP treatment in a concentration-dependent
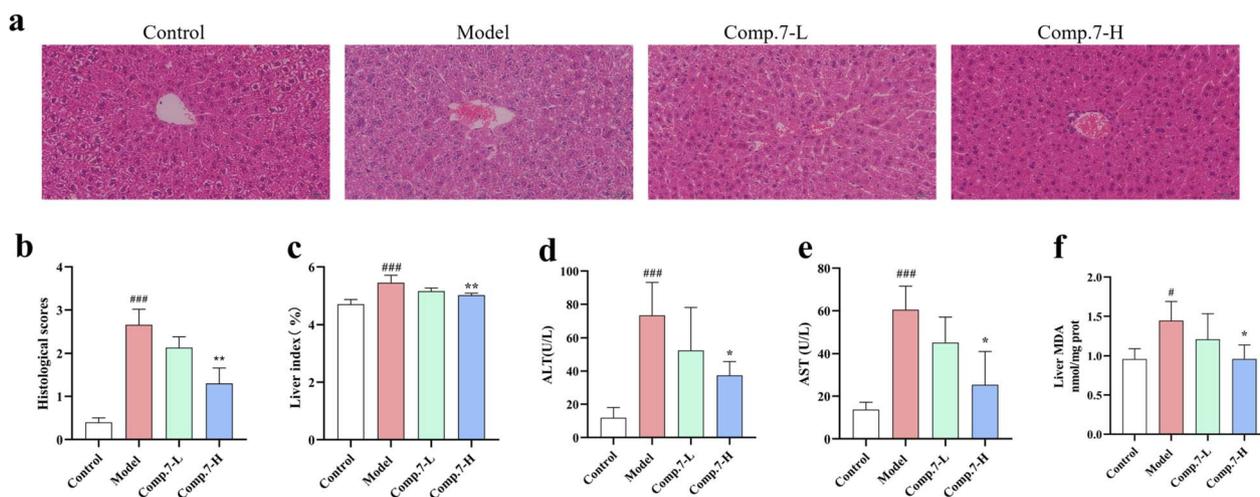


**Fig. 8** Effect of 7 on *t*-BHP-induced hepatotoxicity lesions in mice. (a) H&E staining of hepatic tissue (200× magnification). (b) The histological scores for liver sections. (c) Liver index. (d and e) Serum ALT and AST levels. (f) The levels of MDA in liver tissues. All data are shown as mean ± SD ($n$ = 5). #$p < 0.05$, ##$p < 0.01$, ###$p < 0.001$ *versus* the control group. *$p < 0.05$, **$p < 0.01$, and ***$p < 0.001$ *versus* the model group.

manner, indicating that **7** had an obvious hepatoprotective effect. *t*-BHP has previously been shown to cause oxidative damage. MDA is an end product of lipid peroxidation and a generally accepted marker of oxidative stress.[41] As shown in Fig. 8f, a significant increase in liver oxidation products (MDA) was observed in the model group ($p < 0.05$), whereas those parameters were extremely decreased by **7** pretreatments ($p < 0.01$). These results revealed that **7** pretreatment effectively alleviated oxidative stress in the liver, indicating that the hepatoprotective activity of **7** is related to its antioxidative capacity.

To the best of our knowledge, this is the first report documenting the *in vivo* hepatoprotective activity of **7**, suggesting that **7** serves as the pharmacological basis and primary bioactive constituent responsible for the hepatic protective properties of *I. serra*.

## Conclusion

In conclusion, the total polyphenol (TP) fraction of *I. serra* exhibited pronounced antioxidant activity, attributable to its high phenolic content, and showed superior hepatoprotective effects against *t*-BHP-induced hepatotoxicity compared with the EE and AS fractions. Bioassay-guided fractionation of the TP fraction led to the isolation of two new polyphenols, labiserins A and B (**1** and **2**), together with eight known compounds (**3–10**). Among these, **7** displayed the strongest antioxidant activity, exhibiting nearly tenfold greater radical-scavenging potency than vitamin C in the DPPH assay. Given the critical role of oxidative stress in the pathogenesis of liver injury and the pronounced antioxidant capacity of **7**, its hepatoprotective effects were further evaluated using *in vitro* and *in vivo* models of *t*-BHP-induced liver injury. In HepG2 cells, pretreatment with **7** enhanced SOD activity and reduced ROS and MDA accumulation, thereby alleviating oxidative stress-induced cytotoxicity. Importantly, qRT-PCR analysis further indicated that the hepatoprotective effects of **7** are associated with transcriptional modulation of Keap1, suppression of NF-κB signaling, and consequent downregulation of pro-inflammatory cytokines, including IL-6 and IL-1β, highlighting coordinated regulation of oxidative stress and inflammatory responses as a key component of its hepatoprotective mechanism. Current research demonstrates that **7** is a potential hepatoprotective candidate drug, and it may further serve as a quality marker for *I. serra* in subsequent studies.

## Materials and methods

### General experimental procedures

Optical rotations were measured with a Rudolph Research Analytical Autopol I automatic polarimeter. Ultraviolet (UV) was carried out on a Yokechina double-beam ultraviolet-visible spectrophotometer. IR spectra were measured with a Bruker TEN-SOR37 infrared spectrometer (KBr). HR-ESI-MS spectra analyses were conducted using an Agilent 1290 Infinity LC and Agilent 6530 Q-TOF mass spectrometer (Agilent, Palo Alto, USA). Ultra Performance Liquid Chromatography (UPLC) was performed on the Waters XSelect Premier HSS T3 column (100 mm

$\times$ 2.0 mm, 2.2 μm). 1D and 2D NMR spectra were acquired on a Bruker Ascend 600 NMR spectrometer with TMS as an internal reference. Medium-pressure liquid chromatography (MPLC) was performed using an RP-18 column (YMC $C_{18}$, 46 $\times$ 60 mm, 40–60 μm particle size) on an RUIHE LC-2100 liquid chromatography instrument. Semi-preparative HPLC was conducted on an RUIHE LC-2010 liquid chromatography instrument with a Waters Xbridge or XSelect Prep $C_{18}$ column (10 $\times$ 250 mm, 5 μm).

### Materials and chemicals

The aerial parts of *I. serra* were collected from Qingyuan City of Guangdong Province, as previously described.[42] A voucher specimen (IS-2021-10) has been deposited at the School of Traditional Chinese Materia Medica, Guangdong Pharmaceutical University.

Ethanol, petroleum ether, and ethyl acetate were acquired from Ghtech (Guangzhou, China). The HPLC-grade solvents (methanol and acetonitrile) were obtained from Thermo Fisher Scientific (Suwanee, GA, USA). Methanol-D4 (CD4O) and *tert*-butyl hydroperoxide (*t*-BHP) were obtained from Shanghai Macklin Biochemical Technology Co., Ltd (Shanghai, China). Dimethyl sulfoxide (DMSO), 3-(4,5-dimethylthiazol-2-yl)-2,5-diphenyltetrazolium bromide (MTT), DPPH (2,2-diphenyl-1-picrylhydrazyl) radical scavenging activity assay kit, superoxide dismutase (SOD) assay kit, reactive oxygen species (ROS) assay kit, and total phenols test kit were purchased from Beijing Solarbio Science & Technology Co., Ltd (Beijing, China). Phosphate buffer saline (PBS), Dulbecco's modified Eagle medium (DMEM), 0.25% Trypsin-Ethylene diamine tetraacetic acid (EDTA) solution, and penicillin-streptomycin solution were purchased from Wuhan Servicebio Technology Co., Ltd (Wuhan, China). Fetal bovine serum (FBS) was obtained from Gibco (Waltham, MA, USA). A lipid oxidation (MDA) assay kit and a ferric reducing antioxidant power (FRAP) assay kit were bought from Beyotime (Shanghai, China).

### Extraction and isolation

The initial extraction was previously described.[42] The AS part was subjected to a microporous resin column (D101) by eluting with 20%, 40%, and 60% ethanol, which were combined and vacuum freeze-dried to obtain total polyphenols (TP).[43] The partial TP fraction (20 g) was isolated by MPLC (ODS $C_{18}$, 50 μm) and eluted with MeOH-$H_2O$ (0 : 100 → 100 : 0, v/v) to obtain six fractions (Fr. A to F). Fr. A was separated on RP-HPLC ($CH_3CN$-0.1%FA in $H_2O$, 15 : 85) to obtain **3** (4.72 mg), **4** (3.17 mg), and **5** (2.04 mg). Fr. B ($CH_3CN$−0.1%FA in $H_2O$, 17 : 83) was separated to obtain **6** (4.65 mg). Fr. C ($CH_3CN$-0.1%FA in $H_2O$, 23 : 77) was separated to obtain **7** (600 mg). Fr. D was separated on semi-preparative reversed-phase HPLC (MeOH : 0.1%FA in $H_2O$ = 45 : 55) to obtain **1** (2.32 mg), **9** (14.5 mg), and **10** (4.5 mg). Fr. E was purified by RP-HPLC ($CH_3CN$-0.1%FA in $H_2O$, 30 : 70) to obtain **8** (1.65 mg). Fr. F was purified by RP-HPLC (MeOH-0.1% FA in $H_2O$, 50 : 50) to obtain **2** (3.56 mg).

**Labiserin A (1).** White amorphous powder; UV (MeOH) $\lambda_{max}$ (log $\varepsilon$) 197 (3.31), 261 (2.86), 299 (2.51); IR (KBr) $\nu_{max}$: 3400, 2924,

1701, 1608, 1386, 1275 cm$^{-1}$; $^1$H and $^{13}$C NMR, see Table 1; HR-ESI-MS $m/z$ 305.0657$[M + H]^+$ (Calculated for $C_{15}H_{13}O_7$, 305.0656).

**Labiserin B (2).** Pale yellowish amorphous powder; $[\alpha]$22.3 D -0.013 ($c$ = 0.4, MeOH); UV (MeOH) $\lambda_{max}$ (log $\varepsilon$) 204 (4.10), 238 (3.48), 281 (3.13); IR (KBr) $\nu_{max}$: 3444, 2937, 1731, 1603, 1516, 1454, 1263, 1214, 1141, 1024 cm$^{-1}$; $^1$H and $^{13}$C NMR, see Table 1; HR-ESI-MS $m/z$ 571.1783 $[M + Na]^+$ (Calculated for $C_{27}H_{32}O_{12}Na$, 571.1786).

## ECD calculations

The ECD calculation for **2** was carried out using a previously reported method.[42] Briefly, conformational analyses were conducted using random searching in Spartan 16 (Wavefunction, Irvine, CA, USA, 2016) with the MMFF94 force field. The resulting conformers were re-optimized at the B3LYP/6-31G(d,p) level using DFT and the SMD solvation model in Gaussian 09. For conformers with a Boltzmann population over 1%, energies, oscillator strengths, and rotational strengths were calculated $via$ TDDFT at the B3LYP/6-311+G(d,p) level in methanol. ECD spectra were simulated by applying Gaussian functions (sigma = 0.30) and averaged according to Boltzmann-weighted populations based on relative Gibbs free energies ($\Delta G$).

## Determination of total phenols content (TPC)

The TPC of EE, PE, EA, AS, and TP fractions was evaluated by a total phenols test kit, following the colorimetric method described.[44] About 1 mg of dried powder was weighed, 1 mL of extract solution was added, and the total phenols were extracted by ultrasonic extraction for 30 min. The absorbance of the extraction was measured at a wavelength of 760 nm using a Microplate reader. TPC was expressed as gallic acid equivalents (GAE), which were determined from a gallic acid standard curve (0.01–0.625 mg mL$^{-1}$), and the results were expressed as mg GAE per g sample.

## DPPH radical scavenging activity assay

The DPPH radical scavenging activity assay was determined by using the BC4750 kit, with minor modifications to the protocol as described.[45] Firstly, Reagent II was dissolved with Reagent I. Then, the working solution containing Reagent II and Reagent I (1 : 9, v : v) was prepared before use. Then, 50 μL of prepared samples and standard (vitamin C) of 0.25–5 mM were added to 150 μL of the DPPH solution. The mixture was vortexed to mix and incubated in darkness for 30 min. The absorbance of the reaction mixture was monitored at 515 nm using a multifunctional microplate reader with ethanol being used as the blank. The analysis of each sample was evaluated in triplicate, and the results were expressed as the inhibition rate (%) and EC$_{50}$ values. The DPPH free radical scavenging activity was calculated and expressed as follows:

$$\text{DPPH radical scavenging activity (\%)} = [[(A_0 - (A_1 - A_c)]/A_0] \times 100\%$$

where $A_0$ is the blank absorbance, $A_c$ is the control absorbance, and $A_1$ is the sample/standard control absorbance.

## Ferric reducing antioxidant power (FRAP) assay

The FRAP analysis was evaluated by using the S0116 kit according to the previous method, with some slight modifications.[46] Firstly, a working solution, FRAP reagent, was prepared and heated to 37 °C. FeSO$_4$·7H$_2$O dissolved in water (0.15, 0.3, 0.6, 0.9, 1.2, and 1.5 mM) was used to establish a standard curve. Then, 190 μL of FRAP working solution was mixed with 5 μL of the sample in a 96-well plate. After incubating at 37 °C for 5 min, the absorbance of the mixture was monitored by a microplate reader at 593 nm, with all tests performed in triplicate. Eventually, the total antioxidant capacity was expressed as FeSO$_4$ equivalents, calculated from the standard curve.

## HPLC analysis of the TP fraction

The TP fraction (5 mg) was suspended in distilled water (20 mL) and sonicated for 30 min. After centrifugation at 2000 rpm for 10 min, the supernatant was filtered through a 0.45 μm membrane. The subsequent filtrate was then analyzed using an LC-20AT HPLC system (Shimadzu, Nakagyo-ku, Kyoto, Japan) equipped with a UV detector. HPLC was achieved using a 5 TC-C$_{18}$ (2)-C$_{18}$ column (250 mm × 4.6 mm, 5 μm; Agilent, Santa Clara, CA, USA) with a gradient elution program at a flow rate of 1.0 mL min$^{-1}$. The mobile phase was composed of 0.01% formic acid (A) and acetonitrile (B), and the following gradient was applied: 0–5 min, 95% A; 5–8 min, 95–88% A; 8–20 min, 88–84% A; 20–55 min, 80–67% A. The column temperature was maintained at 35 °C, the detection wavelength was set at 254 nm, and the sample injection volume was 10 μL. Representative chromatograms of the TP fraction were analyzed using a Shimadzu system.

## Cell culture

The human hepatocellular carcinoma cell line (HepG2) was obtained from the American Type Culture Collection (ATCC, Manassas, VA, USA). The HepG2 cells were cultured in DMEM medium supplemented containing 10% FBS and 1% antibiotics (penicillin and streptomycin) in a humidified incubator containing 5% CO$_2$ at 37 °C.

## t-BHP toxicity assay

HepG2 cells ($3 \times 10^3$ cells/well) were cultured in 96-well plates and then exposed to a series of $t$-BHP concentrations (0, 100, 200, 300, 400, and 500 μM) for 2 h, respectively. After the treatment, MTT solution was added and incubated for 4 h at 37 °C in an atmosphere of 5% CO2. DMSO (100 μL/well) was added to dissolve the formazan after the supernatant medium was removed. Finally, absorbance was detected at 490 nm using a microplate reader (Multiskan SkyHigh, Thermo Scientific Co., Ltd, GA, USA).

## Cytoprotective effects assay

HepG2 cells ($1 \times 10^3$ cells/well) were seeded in 96-well plates for measurement of hepatoprotective activity. After attachment, the cells were pretreated with five fractions (EE, PE, EA, AS, and TP) and various concentrations of isolated **7** (0, 20, 40, and 80 μM) for 24 h. Controls received an equal concentration of vehicle (DMSO). Subsequently, the cells were treated with or without 300 μM $t$-BHP to induce oxidative stress. After 2 h of incubation, cell viability was measured by MTT assay as described in the literature.[47] MTT solution was added to the cells and incubated for an additional 4 h. To measure the proportion of surviving cells, the medium was replaced with 100 μL of DMSO. Absorbance was measured at 490 nm with a microplate reader (Multiskan SkyHigh, Thermo Scientific Co., Ltd, GA, USA).

## Measurement of intracellular ROS levels

The intracellular ROS levels were monitored with the fluorescent probe DCFH-DA, as a substrate, as described previously.[48] HepG2 cells ($10^5$ cells/well) were plated in 24-well plates. After incubation with **7** (0, 20, 40, and 80 μM) for 24 h, the cells were treated with or without $t$-BHP (300 μM) for 2 h. Subsequently, the cells were incubated with DCFH-DA probes (10 μM) for 30 min and then were washed three times with PBS. Finally, the fluorescence intensity was measured using flow cytometry (Beckman Coulter, CytoFLEX) (excitation, 488 nm; emission, 525 nm).

## Real-time PCR analysis

HepG2 cells were pre-incubated with **7** (0, 20, 40, and 80 μM) or silymarin (100 μM) for 24 h before exposure to $t$-BHP (300 μM) for 2 h. Cellular RNAs were extracted using the TRIZOL reagent (#RN001, ESscience). Subsequently, cDNA was synthesized (#AT341, TransGen Biotech), and real-time PCR was performed. Relative expression of target genes was normalized to GAPDH, analyzed by $2^{-\Delta\Delta C_t}$ method, and presented as a ratio relative to the control. The primer sequences are shown in Table S3.

## Measurement of intracellular MDA and SOD levels

To measure the MDA and SOD contents in HepG2 cells, the cells ($2 \times 10^5$ cells/well) were cultured in six-well plates. After attachment, cells were pretreated with **7** (0, 20, 40, and 80 μM) for another 24 h and then incubated with or without $t$-BHP (300 μM, 2 h). After washing the cells three times with pre-cooling PBS, the cells were harvested and lysed in an ultrasonic bath. The MDA and SOD contents were determined using the cell MDA assay kit and SOD assay kit. Data for T-SOD was expressed as specific activity units per milligram of protein (U mg$^{-1}$ prot), and MDA was expressed in millimol per milligram of protein (nmol mg$^{-1}$ prot).

## Animals and experimental protocols

Male C57 BL/6 mice aged 6–8 weeks were obtained from Guangzhou Ruige Biological Technology Co., Ltd no. SCXK 2023-0059, Guangzhou, China. Animal study protocols were reviewed and approved by the Ethics Committee of Guangdong Pharmaceutical University no. gdpulacspf2022309. The animal studies were conducted in compliance with the ARRIVE Animal Research: Reporting of *In Vivo* Experiments guidelines.[49] The animals were housed in a dedicated pathogen-free animal facility maintained at a temperature of 22 °C ± 2 °C and relative humidity of 50 ± 5%, with controlled light–dark cycles lasting for 12 hours each. After adopting feed for a week, the mice were administered the following treatments. Mice were randomly divided into the following four groups ($n = 5$): control, model, low-dose **7** (Comp.7 L) group, and high-dose **7** (Comp.7 H) group. The Comp.7 L and Comp.7 H groups were administered 50 mg kg$^{-1}$ and 100 mg kg$^{-1}$ Comp.7 H (dissolved in saline) for 3 consecutive days. Saline was administered to mice in the control and model groups once daily. Three hours after the final administration, the mice were treated with intraperitoneal administration of saline or 3 mmol kg$^{-1}$ $t$-BHP and then sacrificed to collect blood and liver after 24 h.

## Histopathologic evaluation of the liver tissue

To evaluate histological alterations in the liver tissue, the tissues were washed with cold phosphate-buffered saline (PBS) and subsequently fixed in 4% paraformaldehyde. After paraffin embedding, sections were cut at 4 μm slices and stained with hematoxylin and eosin (H&E). The liver tissue was examined under a light microscope to assess pathological alterations.

## Measurement of biochemical parameters and MDA level in liver tissue

The levels of serum ALT and AST were carried out referring to the previous method using corresponding assay kits[50] (Nanjing Jiancheng Bioengineering Institute, Nanjing, China). MDA levels of liver tissues were determined following the Lipid Peroxidation MDA Assay Kit. Briefly, 100 mg of liver tissue was added to 1 ml PBS and homogenized for a few minutes, followed by centrifugation at 1000 rpm for ten minutes. The supernatant was measured using a lipid oxidation (MDA) assay kit, and the MDA content was expressed as nmol mg$^{-1}$ prot.

## Statistical analysis

The data were expressed as means ± SD. Statistical analysis was conducted using a one-way analysis of variance (ANOVA) with GraphPad Prism, Version 8.2.1 (GraphPad Software, Inc., San Diego, CA, USA). Differences were considered significant at $p < 0.05$.

## Author contributions

## Conflicts of interest

There are no conflicts to declare.

## Data availability

## Acknowledgements

## Notes and references

1 P. Banerjee, N. Gaddam, V. Chandler and S. Chakraborty, *Am. J. Pathol.*, 2023, **193**, 1400–1414.

2 Y. Hong, A. Boiti, D. Vallone and N. S. Foulkes, *Antioxidants*, 2024, **13**, 312.

3 E. Ramos-Tovar and P. Muriel, *Antioxidants*, 2020, **9**, 1279.

4 H. A. Hassan, in *The Liver*, ed V. B. Patel, R. Rajendram and V. R. Preedy, Academic Press, Boston, 2018, DOI: 10.1016/B978-0-12-803951-9.00011-2, pp. 121–130.

5 U. Bhuyan and J. G. Handique, *Stud. Nat. Prod. Chem.*, 2022, **75**, 243–266.

6 C. M. C. Andrés, J. M. Pérez de la Lastra, C. A. Juan, F. J. Plou and E. Pérez-Lebeña, *Int. J. Mol. Sci.*, 2024, **25**, 2600.

7 P. Zare Mehrjerdi, S. Asadi, E. Ehsani, V. R. Askari and V. Baradaran Rahimi, *Naunyn-Schmiedeberg's Arch. Pharmacol.*, 2024, **397**, 7531–7549.

8 R. Fuccelli, R. Fabiani and P. Rosignoli, *Molecules*, 2018, **23**, 3212.

9 H. H. Xing, L. J. An, Z. T. Song, S. S. Li, H. M. Wang, C. Y. Wang, J. Zhang, M. Tuerhong, M. Abudukeremu, D. H. Li, D. H. Lee, J. Xu, N. Lall and Y. Q. Guo, *J. Nat. Prod.*, 2020, **83**, 2844–2853.

10 E. S. Bae, Y. M. Kim, D. H. Kim, W. S. Byun, H. J. Park, Y. W. Chin and S. K. Lee, *J. Biomol. Res. Therapeut.*, 2020, **28**, 465–472.

11 J. Wan, M. Liu, H. Y. Jiang, J. Yang, X. Du, X. N. Li, W. G. Wang, Y. Li, J. X. Pu and H. D. Sun, *Phytochemistry*, 2016, **130**, 244–251.

12 L. Lin, Y. Dong, B. Yang and M. Zhao, *Combinatorial Chemistry & High Throughput Screening*, 2011, **14**, 720–729.

13 S. H. Hassanpour and A. Doroudi, *Avicenna J. Phytomed.*, 2023, **13**, 354–376.

14 C. Sánchez-Moreno, L. Plaza, B. de Ancos and M. P. Cano, *Food Chem.*, 2006, **98**, 749–756.

15 H. J. Zhang, M. Yin, L. Y. Huang, J. Wang, L. X. Gong, J. Liu and B. G. Sun, *J. Food Sci.*, 2017, **82**, 278–288.

16 J. P. Piret, T. Arnould, B. Fuks, P. Chatelain, J. Remacle and C. Michiels, *Biochem. Pharmacol.*, 2004, **67**, 611–620.

17 L. Kraut, R. Mues, A. Speicher, M. Wagmann and T. Eicher, *Phytochemistry*, 1996, **42**, 1693–1698.

18 L. Pieters, T. Debruyne, A. Degroot, G. Mei, R. Dommisse, G. Lemiere and A. Vlietinck, *Magn. Reson. Chem.*, 1993, **31**, 692–693.

19 Y. R. Lu and L. Y. Foo, *Phytochemistry*, 2000, **55**, 263–267.

20 W. S. Feng, X. Y. Zang, X. K. Zheng, Y. Z. Wang, H. Chen and Z. Li, *J. Asian Nat. Prod. Res.*, 2010, **12**, 557–561.

21 H. Y. Wu, J. P. Ke, W. Wang, Y. S. Kong, P. Zhang, T. J. Ling and G. H. Bao, *J. Agric. Food Chem.*, 2019, **67**, 11986–11993.

22 S. K. Sadhu, A. Khatun, P. Phattanawasin, T. Ohtsuki and M. Ishibashi, *J. Nat. Med.*, 2007, **61**, 480–482.

23 Y. Kashiwada, M. Nishizawa, T. Yamagishi, T. Tanaka, G. Nonaka, L. M. Cosentino, J. V. Snider and K. H. Lee, *J. Nat. Prod.*, 1995, **58**, 392–400.

24 L. e. a. GhangTai, *Nat. Prod. Sci.*, 2010, 207–210.

25 E. Le Claire, S. Schwaiger, B. Banaigs, H. Stuppner and F. Gafner, *J. Agric. Food Chem.*, 2005, **53**, 4367–4372.

26 G. Liu and J. He, *J. Dali Univ.*, 2010, **9**, 5–7.

27 Y. Lang, N. Gao, Z. Zang, X. Meng, Y. Lin, S. Yang, Y. Yang, Z. Jin and B. Li, *J. Future Foods*, 2024, **4**, 193–204.

28 G. Świderski, E. Gołębiewska, M. Kalinowska, R. Świsłocka, N. Kowalczyk, A. Jabłońska-Trypuć and W. Lewandowski, *Materials*, 2024, **17**, 2575.

29 T. Tufa, H. Damianakos, G. Zengin, K. Graikou and I. Chinou, *J. S. Afr. Bot.*, 2019, **120**, 157–162.

30 C. M. Spagnol, R. P. Assis, I. L. Brunetti, V. L. B. Isaac, H. R. N. Salgado and M. A. Corrêa, *Spectrochim. Acta, Part A Mol. Biomol. Spectrosc.*, 2019, **219**, 358–366.

31 A. Trifan, K. Skalicka-Woźniak, S. Granica, M. E. Czerwińska, A. Kruk, L. Marcourt, J. L. Wolfender, E. Wolfram, N. Esslinger, A. Grubelnik and S. V. Luca, *J. Ethnopharmacol.*, 2020, **262**, 113169.

32 A. Amić and D. Mastiľák Cagardová, *Int. J. Mol. Sci.*, 2022, **23**, 14497.

33 D. Quy Huong, P. C. Nam, D. T. Quang, S. T. Ngo, T. Duong and N. M. Tam, *ACS Omega*, 2024, **9**, 24071–24081.

34 S. Chen, Q. Li, H. Shi, F. Li, Y. Duan and Q. Guo, *Biomed. Pharmacother.*, 2024, **178**, 117084.

35 M. K. Choi, H. G. Kim, J. M. Han, J. S. Lee, J. S. Lee, S. H. Chung and C. G. Son, *Evid. Based Complement. Alternat. Med*, 2015, **2015**, 517350.

36 J. Wu, R. Huang, D. Jiao, S. Liu, H. Liu and H. Liu, *Int. J. Biol. Macromol.*, 2022, **208**, 453–462.

37 J. L. Xiao, H. Y. Liu, C. C. Sun and C. F. Tang, *Mol. Biol. Rep.*, 2024, **51**, 809.

38 F. Guo, X. Zhuang, M. Han and W. Lin, *Food Funct.*, 2020, **11**, 4485–4498.

39 J.-E. Kim, D.-J. You, C. Lee, C. Ahn, J. Y. Seong and J.-I. Hwang, *Cell. Signal.*, 2010, **22**, 1645–1654.

40 H. Ito, T. Miyazaki, M. Ono and H. Sakurai, *Bioorg. Med. Chem.*, 1998, **6**, 1051–1056.

41 R. Cordiano, M. Di Gioacchino, R. Mangifesta, C. Panzera, S. Gangemi and P. L. Minciullo, *Molecules*, 2023, **28**, 5979.

42 S. Li, F. Liang, D. Huang, H. Wu, X. Tan, J. Ma, C. Wei, S. Wang, Z. Huang, G. Yang, X. He and J. Yang, *Molecules*, 2024, **29**, 2733.

43 Z. Li, H. Zhang, Y. Li, H. Chen, C. Wang, V. K. W. Wong, Z. Jiang and W. Zhang, *Phytomedicine*, 2020, **69**, 153209.

44 Y. Zou, S. K. Chang, Y. Gu and S. Y. Qian, *J. Agric. Food Chem.*, 2011, **59**, 2268–2276.

45 F. W. Muema, Y. Liu, Y. L. Zhang, G. L. Chen and M. Q. Guo, *Antioxidants*, 2022, **11**, 1189.

46 Y. B. Xu, G. L. Chen and M. Q. Guo, *Antioxidants*, 2019, **8**, 296.

47 W. Q. Wang and L. J. Xuan, *Phytochemistry*, 2016, **122**, 119–125.

48 X. H. Feng, H. Y. Xu, J. Y. Wang, S. Duan, Y. C. Wang and C. M. Ma, *Phytomedicine*, 2021, **83**, 153479.

49 N. Percie du Sert, V. Hurst, A. Ahluwalia, S. Alam, M. T. Avey, M. Baker, W. J. Browne, A. Clark, I. C. Cuthill, U. Dirnagl, M. Emerson, P. Garner, S. T. Holgate, D. W. Howells, N. A. Karp, S. E. Lazic, K. Lidster, C. J. MacCallum, M. Macleod, E. J. Pearl, O. H. Petersen, F. Rawle, P. Reynolds, K. Rooney, E. S. Sena, S. D. Silberberg, T. Steckler and H. Würbel, *PLoS Biol.*, 2020, **18**, e3000410.

50 Q. Li, W. Zhang, N. Cheng, Y. Zhu, H. Li, S. Zhang, W. Guo and G. Ge, *Phytomedicine*, 2023, **113**, 154726.